

# Myeloid Endoplasmic Reticulum Resident Chaperone GP96 Facilitates Inflammation and Steatosis in Alcohol-Associated Liver Disease

Anuradha Ratna,<sup>1</sup> Arlene Lim,<sup>1</sup> Zihai Li,<sup>2</sup> Josepmaria Argemi,<sup>3</sup> Ramon Bataller ,<sup>3</sup> Gabriela Chiosis,<sup>4</sup> and Pranoti Mandrekar <sup>1</sup>

Cellular stress-mediated chaperones are linked to liver macrophage activation and inflammation in alcohol-associated liver disease (ALD). In this study, we investigate the role of endoplasmic reticulum (ER) resident stress chaperone GP96/HSP90B1/GRP94, paralog of the HSP90 family, in ALD pathogenesis. We hypothesize that ER resident chaperone, heat shock protein GP96, plays a crucial role in alcohol-associated liver inflammation and contributes to liver injury. We show high expression of GP96/HSP90B1 and GRP78/HSPA5 in human alcohol-associated hepatitis livers as well as in mouse ALD livers with induction of GP96 prominent in alcohol-exposed macrophages. Myeloid-specific GP96 deficient (M-GP96KO) mice failed to induce alcohol-associated liver injury. Alcohol-fed M-GP96KO mice exhibit significant reduction in steatosis, serum endotoxin, and pro-inflammatory cytokines compared with wild-type mice. Anti-inflammatory cytokines interleukin-10 and transforming growth factor  $\beta$ , as well as activating transcription factor 3 and triggering receptor expressed on myeloid cells 2, markers of restorative macrophages, were higher in alcohol-fed M-GP96KO livers. M-GP96KO mice exhibit protection in a model of endotoxin-mediated liver injury *in vivo*, which is in agreement with reduced inflammatory responses during *ex vivo* lipopolysaccharide/endotoxin-stimulated bone marrow-derived macrophages from M-GP96KO mice. Furthermore, we show that liver macrophages from alcohol-fed M-GP96KO mice show compensatory induction of GRP78 messenger RNA, likely due to increased splicing of X-box binding protein-1. Finally, we show that inhibition of GP96 using a specific pharmacological agent, PU-WS13 or small interfering RNA, alleviates inflammatory responses in primary macrophages. **Conclusion:** Myeloid ER resident GP96 promotes alcohol-induced liver damage through activation of liver macrophage inflammatory responses, alteration in lipid homeostasis, and ER stress. These findings highlight a critical role for liver macrophage ER resident chaperone GP96/HSP90B1 in ALD, and its targeted inhibition represents a promising therapeutic approach in ALD. (*Hepatology Communications* 2021;5:1165-1182).

**A**lcohol-associated liver disease (ALD) is characterized by steatosis or fatty liver, steatohepatitis, and fibrosis, which can progress to cirrhosis and hepatocellular carcinoma.<sup>(1)</sup> The mechanisms involved in ALD pathogenesis are complex and multifactorial. They primarily include

*Abbreviations:* 17-DMAG, 17-dimethylaminoethylamino-17-demethoxygeldanamycin; ACOX1, acyl-CoA oxidase-1; AH, alcoholic hepatitis; ALD, alcohol-associated liver disease; ALT, alanine aminotransferase; ASH, alcoholic steatohepatitis; AST, aspartate aminotransferase; ATF4, activating transcription factor 4; BMDM, bone marrow-derived macrophage; CD, cluster of differentiation; CHOP, C/EBP-homologous protein; CPT1a, carnitine palmitoyltransferase 1a; CyP2e1, cytochrome P450 superfamily; eIF2 $\alpha$ , eukaryotic initiation factor 2 $\alpha$ ; ELISA, enzyme-linked immunosorbent assay; ER, endoplasmic reticulum; ERS, endoplasmic reticulum stress; FA, fatty acid; FAS, fatty acid synthase; GP96, glycoprotein 96; GRP78, glucose-regulate protein 78; HCV, hepatitis C virus; H&E, hematoxylin and eosin; HSP, heat shock protein; IL, interleukin; LCAD, long-chain acyl-CoA dehydrogenase; LPS, lipopolysaccharide; Ly6C, lymphocyte antigen 6 complex locus C; MCAD, medium-chain acyl-CoA dehydrogenase; MCP-1, monocyte chemoattractant protein-1; M-GP96KO, myeloid-specific GP96 knock down; mRNA, messenger RNA; NAFLD, nonalcoholic fatty liver disease; NIAAA, National Institute on Alcohol Abuse and Alcoholism; NLRP3, nucleotide-binding domain and leucine-rich repeat containing proteins; PPAR- $\alpha$ , peroxisome proliferator-activated receptor alpha; RT-PCR, real-time polymerase chain reaction; SCD1, stearoyl-CoA desaturase-1; siRNA, small interfering RNA; SREBP-1, sterol regulatory element-binding protein 1; TBP, TATA-box protein; TG, triglyceride; TGF- $\beta$ , transforming growth factor-beta; TLR, toll-like receptor; TNF- $\alpha$ , tumor necrosis factor-alpha; Trem-2, triggering receptor expressed on myeloid cells 2; UPR, unfolded protein response; WT, wild type; XBP-1, X-box binding protein-1.

Received November 17, 2020; accepted March 1, 2021.

acetaldehyde-mediated toxicity, oxidative and endoplasmic reticulum (ER) stress, gut-derived mediators, pro-inflammatory response, and cell death. Currently, there are no Food and Drug Administration–approved therapies for alcoholic hepatitis (AH), and standard of care mostly relies on abstinence, corticosteroids, nutritional support, and liver transplantation for end-stage liver disease.<sup>(1)</sup> Understanding pathogenic mechanisms to identify potential molecular targets during prolonged alcohol exposure is therefore pertinent to develop effective and targeted therapies for ALD.

Exposure of cells to different stressors such as heat shock, toxic chemicals, infections, and alcohol leads to the induction of stress-mediated proteostasis chaperones, also known as heat shock proteins (HSPs).<sup>(2,3)</sup> Highly conserved HSPs are involved in protein homeostasis. When unable to restore homeostasis during chronic cellular stress, HSPs contribute to pathologies including cancer, neurodegenerative diseases, and liver injury. HSP90 is an extensively studied chaperone that plays an important role in disease pathologies. There are four different HSP90 paralogs: inducible HSP90 $\alpha$ /HSP90AA1 and constitutive HSP90 $\beta$ /HSP90AB1 in the cytosol, GP96/HSP90B1 (also called GRP94/ERp99/endoplasmic reticulum chaperone) in the ER, and tumor necrosis factor receptor–associated protein 1 in mitochondria.<sup>(4)</sup>

Chronic insults including alcohol exposure disturb cellular homeostasis and induce HSPs in the ER and cytoplasm.<sup>(5)</sup> Previous studies from our lab reported that cytosolic stress-induced chaperone HSP90AA1 contributes to ALD, and its pharmacological inhibition can reverse liver injury.<sup>(6)</sup> On the other hand, an anti-inflammatory function of cytosolic HSP70/HSPA1A in macrophages and monocytes during moderate alcohol exposure *in vitro* and in humans was also reported by our group.<sup>(3)</sup> Here we sought to determine the role of ER resident HSP90 family chaperone, GP96/HSP90B1, in ALD. Glycoprotein 96 (GP96) is an indispensable ER resident master chaperone required for the folding, processing, and trafficking of several client proteins, including toll-like receptors (TLRs), integrins, Wnt co-receptors, and insulin-like growth factors.<sup>(7)</sup> In response to ER stress, the unfolded protein response (UPR) is activated, resulting in induction of chaperone HSPs, GP96, and GRP78. Various ER stress mediators have been directly linked to hepatic steatosis and inflammation during ALD.<sup>(5,8-10)</sup> However, the role of ER stress-mediated HSP chaperone GP96 in alcohol-induced liver inflammation and injury remains unexplored.

In this study, we investigated induction of GP96/HSP90B1 in human AH livers and evaluated its role

*Additional Supporting Information may be found at [onlinelibrary.wiley.com/doi/10.1002/hep4.1713/suppinfo](https://onlinelibrary.wiley.com/doi/10.1002/hep4.1713/suppinfo).*

*Supported by the National Institute of Alcohol Abuse and Alcoholism (R01 AA17986-01A1 and R01 AA25289-01).*

© 2021 The Authors. *Hepatology Communications* published by Wiley Periodicals LLC on behalf of the American Association for the Study of Liver Diseases. This is an open access article under the terms of the Creative Commons Attribution–NonCommercial–NoDerivs License, which permits use and distribution in any medium, provided the original work is properly cited, the use is non-commercial and no modifications or adaptations are made.

*View this article online at [wileyonlinelibrary.com](https://onlinelibrary.wiley.com).*

*DOI 10.1002/hep4.1713*

*Potential conflict of interest: Dr. Chiosis owns stock and intellectual property rights in Samus Therapeutics. Dr. Li advises Amphamab, Henlius, Ikonisys, and Heat.*

## ARTICLE INFORMATION:

From the <sup>1</sup>Department of Medicine, University of Massachusetts Medical School, Worcester, MA, USA; <sup>2</sup>Division of Medical Oncology, Department of Medicine, Pelotonia Institute for Immuno-Oncology, The Ohio State University Comprehensive Cancer Center, Columbus, OH, USA; <sup>3</sup>Division of Gastroenterology, Hepatology and Nutrition, Pittsburgh Liver Research Center, University of Pittsburgh Medical Center, Pittsburgh, PA, USA; <sup>4</sup>Chemical Biology Program, Memorial Sloan Kettering Cancer Center, New York, NY, USA.

## ADDRESS CORRESPONDENCE AND REPRINT REQUESTS TO:

Pranoti Mandrekar, Ph.D., F.A.A.S.L.D.  
Department of Medicine  
University of Massachusetts Medical School  
Lazare Research Building, Rm 221

364 Plantation Street  
Worcester, MA 01605, USA  
E-mail: [Pranoti.Mandrekar@umassmed.edu](mailto:Pranoti.Mandrekar@umassmed.edu)  
Tel.: +1-508-856-5391

using experimental models in alcohol-induced liver injury. We show that GP96 is significantly increased in human AH livers as well as in murine livers, prominently in macrophages after chronic alcohol administration. We hypothesized that myeloid-specific GP96 plays a crucial role in alcohol-induced inflammation and ALD. To test our hypothesis, we generated myeloid-specific GP96 deficient (M-GP96KO) mice<sup>(11)</sup> and subjected them to two models of alcohol-induced liver injury: 4 weeks of chronic alcohol and National Institute on Alcohol Abuse and Alcoholism (NIAAA)–Gao chronic-binge alcohol model. We demonstrate that myeloid-specific deletion of GP96 prevents chronic alcohol-mediated liver injury, steatosis, and inflammation. Interestingly, we found higher expression of anti-inflammatory genes interleukin (IL) 10 and transforming growth factor  $\beta$  (TGF- $\beta$ ) as well as restorative macrophage markers, activating transcription factor 3 (ATF3), and triggering receptor expressed on myeloid cells 2 (Trem-2). M-GP96KO mice had increased expression of fatty acid (FA) oxidation genes and reduced expression of lipogenic genes in hepatocytes. Furthermore, we show that liver macrophages from alcohol-fed M-GP96KO mice show compensatory induction of GRP78 messenger RNA (mRNA), likely due to increased splicing of X-box binding protein-1 (XBP-1). Finally, we demonstrate that a cell permeable GP96 specific inhibitor, PU-WS13,<sup>(12,13)</sup> and GP96-specific small interfering RNA (siRNA) markedly reduced pro-inflammatory cytokine production in murine primary macrophages, confirming an important role for GP96 in macrophage activation.

## Materials and Methods

### HUMAN LIVER SAMPLES

Human liver tissue samples were obtained from the Human Biorepository Core from National Institutes of Health–funded InTeam consortium (7U01AA021908-05).<sup>(14)</sup> Patients with asymptomatic early stages of alcoholic steatohepatitis (ASH) (early\_ASH, n = 12), severe AH (severe\_AH, n = 17), and explants from AH (explant\_AH, n = 10), who underwent early liver transplantation,<sup>(15)</sup> were included, as previously described,<sup>(14)</sup> and liver biopsies were obtained. Patients with other liver diseases

or malignancies were excluded from the study. These groups were compared with fragments of nondiseased human livers (normal, n = 10) and disease controls (i.e., patients with nonalcoholic fatty liver disease (NAFLD; n = 9), noncirrhotic HCV infection (HCV; n = 10), and compensated HCV-related cirrhosis (comp\_Cirrhosis; n = 9). Clinical characteristics of these patients are summarized in Supporting Table S1.<sup>(14)</sup> RNA extraction, RNA sequencing, and bioinformatic analysis were carried out as described previously.<sup>(14)</sup> Linear model fitting and differential expression analyses were carried out using fit linear models to genes, and the eBayes moderated *t*-statistic was used to assess differential expression.

Samples used for immunohistochemistry were provided by the Liver Tissue Cell Distribution System (Division of Pediatric Gastroenterology and Nutrition, University of Minnesota, Minneapolis, MN). Alcoholic cirrhotic human livers were obtained from patients who underwent transplantation. Normal liver tissue was the noninvolved surrounding tissue obtained from patients undergoing partial hepatectomy for liver cancer. Biochemical profiles of these patients are described in Supporting Table S1.

### ANIMAL EXPERIMENTS

All animal experiments were approved by the Institutional Animal Care and Use Committee of the University of Massachusetts Medical School, and animals received humane care in agreement with the approved protocols. *Hsp90b1<sup>flox/flox</sup>* mice<sup>(11)</sup> were crossed with *LysM<sup>Cre</sup>* mice (Jackson Laboratory, Bar Harbor, ME) to generate *LysM<sup>Cre</sup>Hsp90b1<sup>flox/flox</sup>* (referred as M-GP96KO) and *Hsp90b1<sup>flox/flox</sup>* Cre-negative littermate wild-type (WT) control (all mice on C57BL/6J background). M-GP96KO mice were characterized and GP96 deletion from liver macrophages was confirmed by real-time polymerase chain reaction (RT-PCR) (Supporting Fig. S2A). We isolated neutrophils (Ly6G<sup>+</sup>), as described previously by us,<sup>(16)</sup> from M-GP96KO mice and were found to be responsive to TLR4 ligand (Supporting Fig. S2A), as shown earlier,<sup>(11)</sup> suggesting that granulocytes still express GP96, despite the *Cre* activity, likely due to the rapid turnover of neutrophils and long half-life of GP96.<sup>(11)</sup> To induce liver injury in female M-GP96KO and WT mice (10–25-week-old) mice, we used established models

of ALD and inflammation: 4-week chronic alcohol model,<sup>(17,18)</sup> NIAAA-Gao chronic binge model,<sup>(6,19)</sup> and endotoxin-mediated liver injury model.<sup>(18)</sup> Of the total mice subjected to alcohol-feeding regimens, some animals were perfused for liver cell isolation, whereas serum samples from all animals were used for assays (n = 12-16 mice per group).

## ISOLATION OF HEPATOCYTES AND LIVER MACROPHAGES

Hepatocytes and liver macrophages were isolated following the protocol as described previously.<sup>(20)</sup> The purity of isolated hepatocytes and liver macrophages was determined by evaluating the expression of their respective markers, albumin and Clec4f, by RT-PCR (Supporting Fig. S2A).

## PREPARATION OF NUCLEAR AND MICROSOMAL FRACTIONS

Nuclear extracts were prepared from mouse livers as described previously.<sup>(21)</sup> Microsomal fractions were prepared from liver tissue by differential centrifugation, as described previously.<sup>(6)</sup> Protein content was measured using Bio-Rad Dye Reagent (Hercules, CA).

## CELL CULTURE AND TREATMENT

Mouse bone marrow-derived macrophages (BMDMs) were generated as described previously.<sup>(22)</sup> BMDMs (0.8 million cells/well) were stimulated with 100 ng/mL lipopolysaccharide (LPS; Sigma-Aldrich, St. Louis, MO), 25 mM ethanol, 1  $\mu$ M 17-dimethylaminoethylamino-17-demethoxygeldanamycin (17-DMAG; Invivogen, San Diego, CA), and 0.5  $\mu$ M PU-WS13,<sup>(23)</sup> as indicated. RAW 264.7 cells were transiently transfected with GP96 siRNA (50 nM or 100 nM) or negative siRNA control (Thermo Fisher Scientific, Waltham, MA) using Lipofectamine 2000 (Invitrogen, Carlsbad, CA) for 48 hours and then stimulated with LPS for the final 6 hours. RNA, culture media, and whole cell lysates were collected for the indicated assays. BMDMs were also collected from LPS-injected WT and M-GP96KO mice for cytokine expression analysis using RT-PCR.

## BIOCHEMICAL ASSAYS

Serum levels of alanine aminotransferase (ALT), aspartate aminotransferase (AST) and endotoxin, hepatic triglyceride (TG), and thiobarbituric acid reactive substances (TBARS) levels were determined. Additional details are mentioned in the Supporting Information.

## RNA EXTRACTION AND RT-PCR

Total RNA was isolated from whole liver, isolated liver cells, and BMDMs. The complementary DNA was synthesized and RT-PCR was performed. Primer sequences are listed in Supporting Table S2.

## HISTOLOGY AND IMMUNOHISTOCHEMISTRY

Mouse liver sections were stained with hematoxylin and eosin (H&E) or Oil Red O, analyzed by microscopy and quantitated using ImageJ Software. For immunohistochemistry, liver sections were incubated with GP96 primary antibodies (2104; Cell Signaling Technology, Danvers, MA), followed by incubation with secondary antibody.

## WESTERN BLOT AND ENZYME-LINKED IMMUNOSORBENT ASSAY

Lysates from BMDM, whole liver, and nuclear extract (5-30  $\mu$ g) were resolved on 7.5% or 10% sodium dodecyl sulfate-polyacrylamide gel electrophoresis gels and electroblotted onto either nitrocellulose or polyvinylidene fluoride membrane (Bio-Rad). Antibodies used were GP96 (SMC-105; StressMarq Biosciences, Cadboro, Canada), GRP78 (CST-3183; Cell Signaling Technology), peroxisome proliferator-activated receptor alpha (PPAR- $\alpha$ ) (sc-9000; Santa Cruz Biotechnology, Dallas, TX), CyP2e1 (AB1252; MilliporeSigma, Burlington, MA), calnexin (ab2295; Abcam, Cambridge, United Kingdom), C/EBP-homologous protein (CHOP) (sc-7351; Santa Cruz Biotechnology), ATF6 $\alpha$  (sc-166659; Santa Cruz Biotechnology), ATF4 (10835-1-AP; Proteintech, Rosemont, IL), ATF3 (sc-81189; Santa Cruz Biotechnology),  $\beta$ -actin (ab6276; Abcam), tubulin (ab6046; Abcam), and TATA-box protein (TBP) (ab818, Abcam). Membranes were probed



with corresponding secondary antibodies (Abcam) and detected using a Western ECL substrate kit (Bio-Rad). Densitometric analysis was done using Fiji ImageJ 1.51d. Intracellular cytokine levels were measured in liver whole-cell lysate and BMDM culture supernatants using mouse tumor necrosis factor- $\alpha$  (TNF- $\alpha$ ) (430904; BioLegend, San Diego, CA) and monocyte chemoattractant protein-1 (MCP-1) (432704; BioLegend) enzyme-linked immunosorbent assay (ELISA) kits.

## STATISTICAL ANALYSIS

All data are presented as mean  $\pm$  SEM. Differences between two groups were assessed using a Student *t* test. One or two-way analysis of variance was used to assess differences among multiple groups. Statistical analyses were performed using GraphPad Prism 8.0 (GraphPad, La Jolla, CA) and were considered statistically significant at  $P < 0.05$ .

## Results

### CHRONIC ALCOHOL CONSUMPTION INDUCES GP96 IN HUMAN AH AND EXPERIMENTAL MURINE ALD

GP96/HSP90B1 and GRP78/BiP are induced during UPR.<sup>(7)</sup> Previous studies identify crucial roles for GP96 and GRP78 in metabolic disease<sup>(8,24)</sup> and liver cancer.<sup>(25)</sup> Although Ji and Kaplowitz have studied GRP78 during ALD,<sup>(8)</sup> the role of GP96 is not yet identified. We first assessed the expression of HSP90B1/GP96 and HSPA5/GRP78 in liver biopsies from cohorts of patients with liver disease including ASH, AH, NAFLD, and HCV. Expression of HSP90B1/GP96 was markedly increased in AH livers and explants compared with normal liver (Fig. 1A). Similar to previous reports,<sup>(8)</sup> HSPA5/GRP78 increased significantly in AH livers. We observed high expression of GP96 protein assessed by immunohistochemistry in human alcoholic cirrhosis livers (Fig. 1B). Next, we assessed levels of GP96 and GRP78 in a murine model of ALD. GRP78 mRNA and protein levels increased significantly in whole livers from alcohol-fed WT littermates (Fig. 1C). The mRNA and protein levels of GP96 showed

an increasing trend in alcohol-fed WT littermates (Fig. 1C), whereas the mRNA induction in livers of alcohol-fed C57BL/6J compared with pair-fed controls reached significance (Supporting Fig. S1A).

GP96 and GRP78 protein levels in the liver reflected mRNA levels in alcohol-fed livers (Fig 1D). Next, we found that alcohol significantly induced GP96 expression in liver macrophages, and increasing trends were seen in hepatocytes (Fig. 1E). On the other hand, GRP78 was significantly increased in hepatocytes but not in macrophages (Fig. 1E). To further substantiate macrophage-specific induction of GP96, we isolated BMDM from C57BL/6J mice and exposed them to physiologically relevant concentrations of alcohol (25 mM) *in vitro* at different time intervals. *In vitro*, 25 mM ethanol concentration approximates a 0.1g/dL blood alcohol level (BAC), which is above the legal limit of BAC.<sup>(26)</sup> Significant induction in GP96 mRNA was achieved after 12 hours of alcohol exposure, whereas GRP78 mRNA showed no induction (Fig. 1F). GP96 protein was detected by 48 hours of alcohol exposure (Fig. 1G), and we did not observe induction at lower time points (Supporting Fig. S1B). These results indicate that GP96 is induced by alcohol in human AH livers and in liver macrophages.

### MYELOID-SPECIFIC DELETION OF GP96 ALLEVIATES ALCOHOL-INDUCED LIVER INJURY

Based on the role of GP96 in immune signaling and its significant induction in macrophages of alcoholic livers, we next sought to investigate the role of myeloid-specific GP96 deletion on chronic alcohol-induced liver injury. Using *LysM<sup>Cre</sup>* mice and *Hsp90b1<sup>fllox/fllox</sup>* mice, we generated M-GP96KO mice. For rigorous analysis, two ALD models were used: (1) 4 weeks of chronic alcohol and (2) NIAAA-Gao chronic binge alcohol. Chronic alcohol feeding resulted in liver injury and steatosis, as evidenced by increased liver/body weight ratio (Fig 2A), serum ALT (Fig 2B), TG level (Fig 2C), and H&E staining (Fig. 2D) in WT mice and were significantly attenuated in alcohol-fed M-GP96KO mice (Fig. 2B-D). Consistent with increased TG, we found a significant increase in Oil Red O staining in livers of alcohol-fed WT mice, which was reduced in M-GP96KO mice (Fig. 2E). Furthermore, we observed that M-GP96KO mice

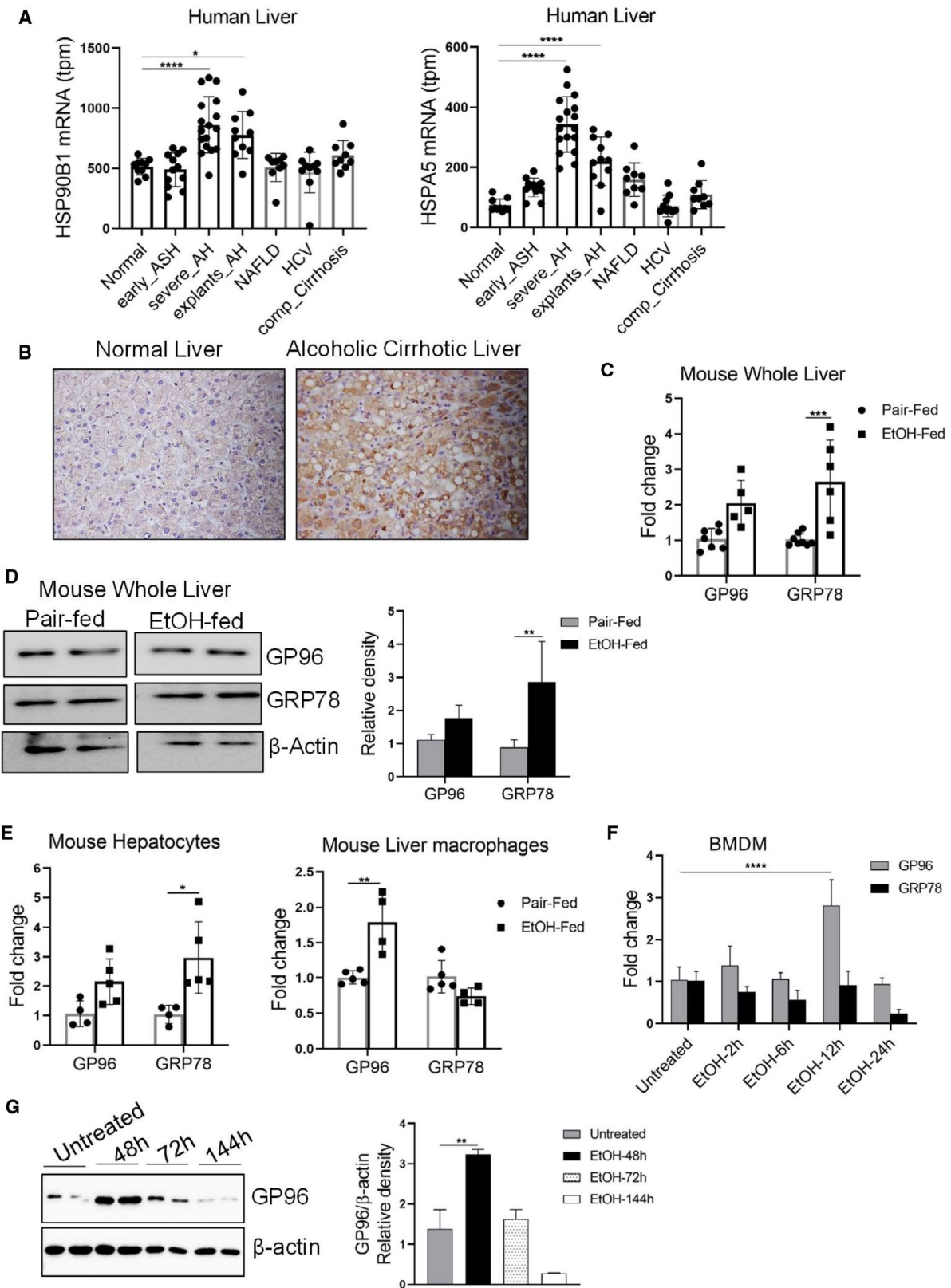


**FIG. 1.** HSP90B1 and HSPA5 genes and GP96 are induced in ALD. (A) mRNA abundance of HSP90B1 and HSPA5 genes (in transcripts per million) was evaluated by RNA sequencing in patients with normal liver (n = 10), early ASH (n = 12), severe\_AH (n = 17), explants\_AH (n = 10), and livers from NAFLD (n = 10), HCV (n = 10), and comp\_Cirrhosis (n = 9). (B) Representative immunohistochemistry of GP96 in human normal and alcoholic liver (magnification  $\times 200$ ). WT mice were fed with control liquid diet (pair-fed) or diet containing 5% alcohol for 4 weeks. The mRNA expression of GP96 and GRP78 was measured by RT-PCR in livers (C) and isolated hepatocytes (E) and liver macrophages (n = 4-10). (D) Protein level of GP96 and GRP78 in liver lysate was analyzed by western blotting (n = 6). (F) BMDMs were treated with 25 mM ethanol and mRNA expression of GP96 and GRP78 (n = 6). (G) The protein level of GP96 was analyzed at different time intervals (n = 3). Data are represented as mean  $\pm$  SEM. \* $P < 0.05$ , \*\* $P < 0.01$ , \*\*\* $P < 0.001$ , \*\*\*\* $P < 0.0001$ . Abbreviations: EtOH, alcohol; comp, compensated; tpm, transcripts per million.

showed a similar protective effect on liver injury in the NIAAA-Gao chronic binge alcohol administration model (Supporting Fig. S2B-F). These studies confirm that GP96 deletion in macrophages prevents alcohol-induced liver injury.

### MYELOID-SPECIFIC GP96 IS CRUCIAL IN ALCOHOL-MEDIATED LIPID METABOLISM

Prolonged alcohol exposure leads to increased TG through reduction in  $\beta$ -oxidation of FA and simultaneous enhancement of lipogenesis in hepatocytes.<sup>(27)</sup> Based on decreased TG in alcohol-fed M-GP96 livers, we investigated whether myeloid-specific GP96 deletion reduces steatosis through regulation of lipid homeostasis genes. We evaluated hepatocyte mRNA abundance of PPAR- $\alpha$ , an important transcription factor that drives FA oxidation, and its target genes: carnitine palmitoyltransferase 1a (CPT1a), acyl-CoA oxidase-1 (ACOX1), long-chain acyl-CoA dehydrogenase (LCAD), and medium-chain acyl-CoA dehydrogenase (MCAD). Alcohol-exposed M-GP96KO livers exhibit increased nuclear PPAR- $\alpha$  protein level compared with WT counterparts (Fig. 3A). Expression levels of PPAR- $\alpha$ , downstream target gene CPT1a, was significantly increased in hepatocytes of alcohol-fed M-GP96KO mice with trends of high LCAD and MCAD mRNA in M-GP96KO hepatocytes but no change in ACOX1 mRNA level (Fig. 3B-E). Concomitantly, we found significant down-regulation of chronic alcohol-induced lipogenic target genes sterol regulatory element-binding protein 1 (SREBP1), stearoyl-CoA desaturase-1 (SCD-1), and fatty acid synthase (FAS) in hepatocytes of alcohol-fed M-GP96KO mice (Fig. 3F-H). Together, our results indicate elevated FA oxidation genes and reduced lipogenesis in hepatocytes from alcohol-fed M-GP96KO mice, identifying mechanisms related to reduced steatosis.

### MYELOID-SPECIFIC GP96 DEFICIENCY INHIBITS PRO-INFLAMMATORY CYTOKINE PRODUCTION

Alcohol consumption is linked to gut permeability and increased leakage of endotoxin in circulation.<sup>(28)</sup> In addition, alcohol metabolism induces oxidative stress sensitizing liver macrophages to endotoxin, resulting in a pro-inflammatory profile in the liver. Chronic alcohol exposure led to significant elevation in serum endotoxin/LPS levels, which was significantly reduced in M-GP96KO mice (Fig 4A). Interestingly, microsomal Cyp2e1 level, an alcohol-metabolizing enzyme linked to oxidative stress, was similar in livers of alcohol-fed M-GP96KO and WT mice (Fig. 4B), suggesting that myeloid-specific GP96 deficiency did not alter alcohol metabolism. We found that chronic binge alcohol exposure also showed similar levels of Cyp2e1 in WT and M-GP96KO livers, whereas oxidative stress marker TBARS was significantly decreased in alcohol-fed M-GP96KO livers (Supporting Fig. S3A, B). Next, we observed that elevated expression of pro-inflammatory cytokines TNF- $\alpha$ , IL-6, IL-1 $\beta$ , and MCP-1 in WT alcoholic livers was significantly inhibited in M-GP96KO mice in both ALD models (Fig. 4C and Supporting Fig. S3C). We also found a significant decrease in nucleotide-binding domain and leucine-rich repeat containing proteins (NLRP3) expression in alcohol-fed M-GP96KO livers, concomitant to reduced IL-1 $\beta$ , supporting decreased LPS/TLR4 responses. Interestingly, mRNA expression of anti-inflammatory restorative macrophage markers, IL-10, TGF- $\beta$ , and ATF3 was high in alcohol-fed M-GP96KO livers (Fig. 4C). Interestingly, deletion of myeloid GP96 itself significantly induced protein and mRNA levels of ATF3 compared with WT whole livers, indicating phenotypic change in liver macrophages of M-GP96KO mice (Fig. 4E and Supporting Fig. S3H). Analysis of representative pro-inflammatory



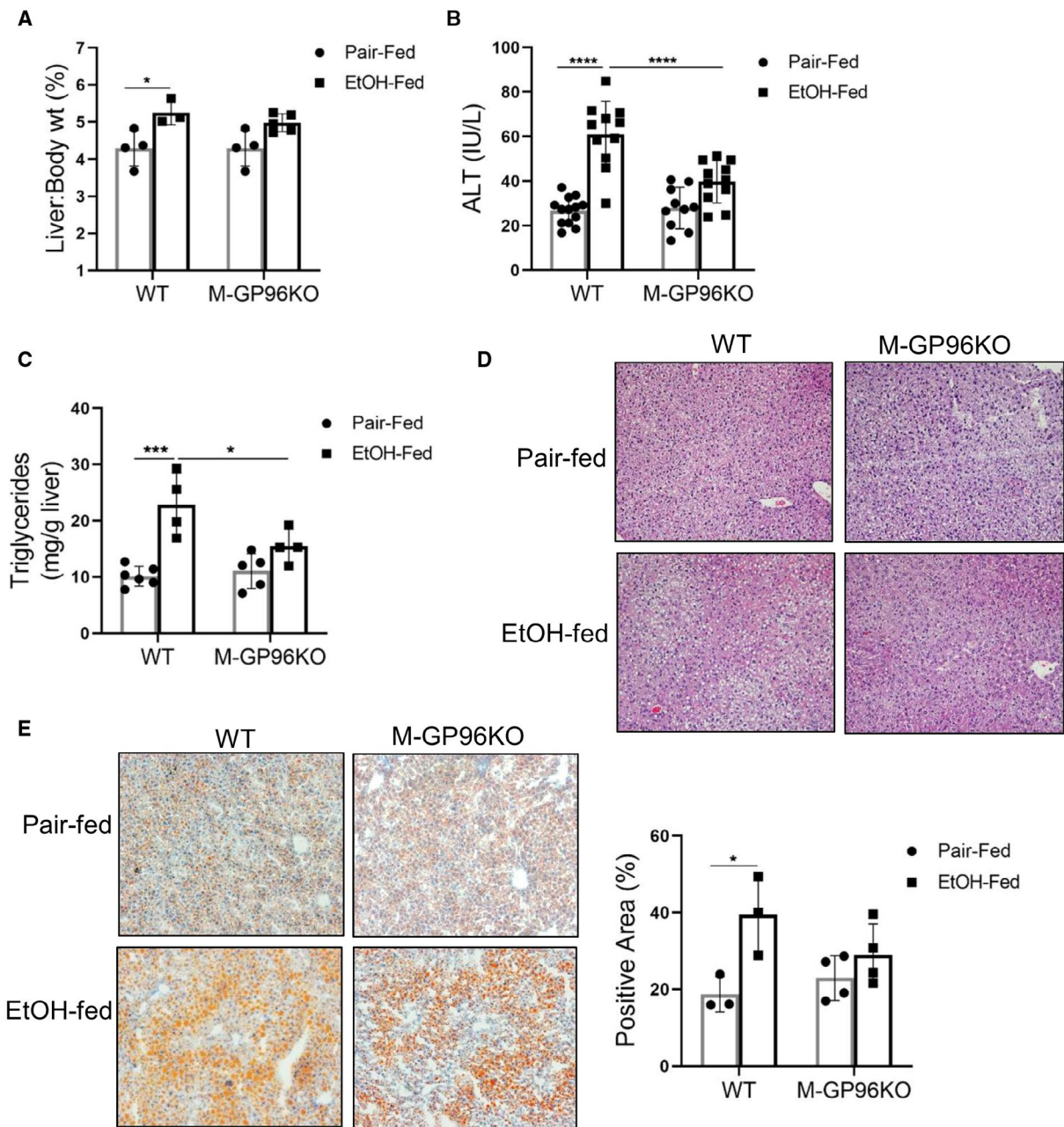


**FIG. 2.** Myeloid-specific GP96 deficiency alleviates chronic alcohol-induced liver injury. Female WT and M-GP96KO mice were fed with isocaloric control liquid diet (pair-fed) or 5% alcohol-containing Leiber-DeCarli diet (alcohol-fed) for 4 weeks, and liver-to-body weight ratio (A), serum levels of ALT (n = 10-16) (B), and liver triglycerides (C) were analyzed. Representative photomicrographs of hepatic injury and steatosis assessed by H&E (D) and Oil Red O (E) staining in livers of mice of the indicated genotype (magnification × 100). Percentage of Oil Red O–positive area was quantitated by ImageJ (n = 3-6). Data are presented as mean ± SEM. \**P* < 0.05, \*\**P* < 0.01, \*\*\**P* < 0.001, \*\*\*\**P* < 0.0001. Abbreviations: EtOH, alcohol; wt, weight.

cytokines, TNF- $\alpha$ , and MCP-1 protein by ELISA showed lack of induction in alcohol-fed M-GP96KO livers compared with the corresponding pair-fed control mice and WT counterparts (Fig. 4D and Supporting

Fig. S3D, E), suggesting decreased pro-inflammatory responses in these livers. Furthermore, investigation of macrophage markers demonstrated marked reduction in alcohol-fed M-GP96KO mice livers (Fig. 4F



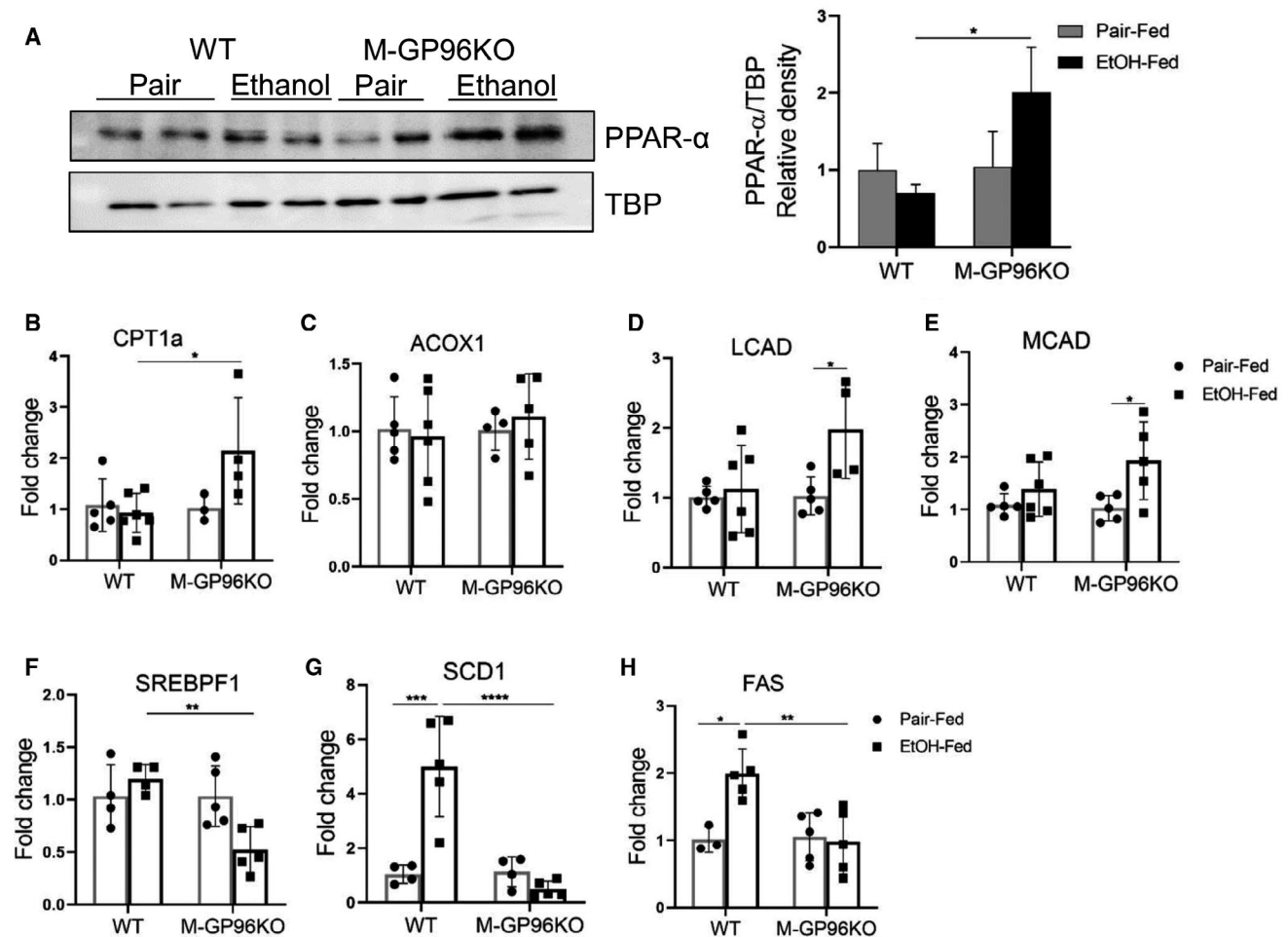


**FIG. 3.** Mice lacking myeloid-specific GP96 exhibit altered lipid metabolism after 4 weeks of alcohol consumption. (A) PPAR- $\alpha$  protein was detected in nuclear extracts of livers by western blot, and expression was quantitated and normalized to pair-fed group ( $n = 4$ ). TBP was used as loading control. The mRNA expression of genes involved in fatty acid  $\beta$ -oxidation (CPT1a, ACOX1, LCAD, and MCAD) (B-E) and lipogenesis (SREBPF1, SCD1, and FAS) (F-H) was analyzed in WT and M-GP96KO hepatocytes by RT-PCR and compared with pair-fed control ( $n = 3-6$ ). Data are presented as mean  $\pm$  SEM. \* $P < 0.05$ , \*\* $P < 0.01$ , \*\*\* $P < 0.001$ , \*\*\*\* $P < 0.0001$ .

and Supporting Fig. S3F). Earlier studies showed that GP96 serves as a chaperone for TLR4 surface expression.<sup>(29)</sup> We next evaluated pro-inflammatory cytokine mRNA profile in isolated liver macrophages as well as in BMDMs treated with LPS *in vitro*. Alcohol-induced mRNA expression levels of several pro-inflammatory cytokines and NLRP3 was reduced in liver macrophages of the alcohol-fed M-GP96KO group (Fig. 4G). Trem-2, expressed on Kupffer cells (KCs), has been proposed to attenuate TLR4-mediated inflammation and limit hepatic injury.<sup>(30)</sup> Increased expression of TGF- $\beta$ , Trem-2, and ATF3 were indicative of anti-inflammatory restorative macrophages in alcohol-fed M-GP96KO mice (Fig. 4H). Reduction

in pro-inflammatory cytokines was also confirmed in LPS-treated BMDMs from M-GP96KO mice (Fig. 4I). Supporting earlier findings that endosomal TLR3 does not require GP96,<sup>(29)</sup> we noted that BMDMs from M-GP96KO mice remained responsive to TLR3 ligand, polyI:C, and produced high levels of pro-inflammatory cytokines (Supporting Fig. S3G). It has been previously reported that the differentiation and survival of GP96-deficient macrophages is uncompromised, and they can be activated through other immune pathways using TNF- $\alpha$ , IL-1 $\beta$ , and IFN- $\gamma$ .<sup>(11)</sup> Our results clearly confirm that macrophages in the liver and bone marrow-derived lacking GP96 exhibit a reduced pro-inflammatory gene profile.

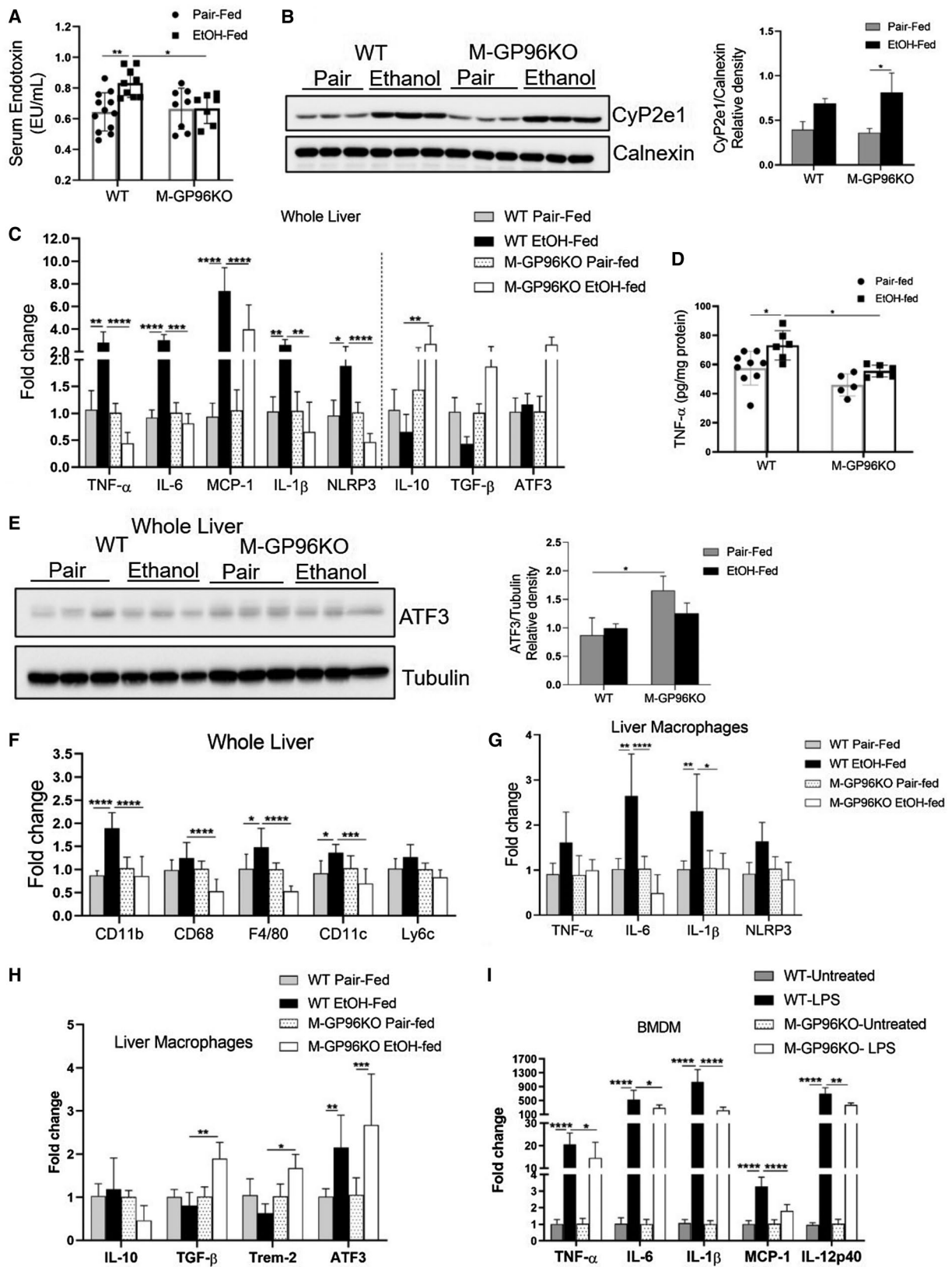


**FIG. 4.** Myeloid-specific GP96 deficiency prevents chronic alcohol-induced endotoxin and pro-inflammatory cytokine production. (A) Endotoxin level was measured in serum ( $n = 8-12$ ). (B) Cyp2e1 was detected in liver microsomal fraction by western blot, and calnexin was used as an internal loading control ( $n = 3$ ). Total RNA from liver tissue was subjected to quantitative RT-PCR for analysis of pro-inflammatory cytokines TNF- $\alpha$ , IL-6, MCP-1, and IL-1 $\beta$ ; NLRP3; anti-inflammatory markers IL-10, TGF- $\beta$ , and ATF3 (C); and macrophage markers ( $n = 6-10$ ) (F). (D) Total liver protein level for TNF- $\alpha$  was measured in tissue extracts of pair-fed and alcohol-fed mice by ELISA ( $n = 6-10$ ). (E) ATF3 protein level was analyzed by western blot in whole-liver extracts using tubulin as an internal control ( $n = 3$ ). The mRNA expression profile of (G) pro-inflammatory, and (H) anti-inflammatory and restorative macrophage markers, Trem2 and ATF3, were analyzed in liver macrophages of pair-fed and alcohol-fed mice ( $n = 5$ ). (I) The mRNA level of pro-inflammatory cytokines was analyzed in BMDMs isolated from WT and M-GP96KO mice and stimulated with 100 ng/mL LPS for 2 hours ( $n = 9$ ). Data are represented as mean  $\pm$  SEM. \* $P < 0.05$ , \*\* $P < 0.01$ , \*\*\* $P < 0.001$ , \*\*\*\* $P < 0.0001$ .

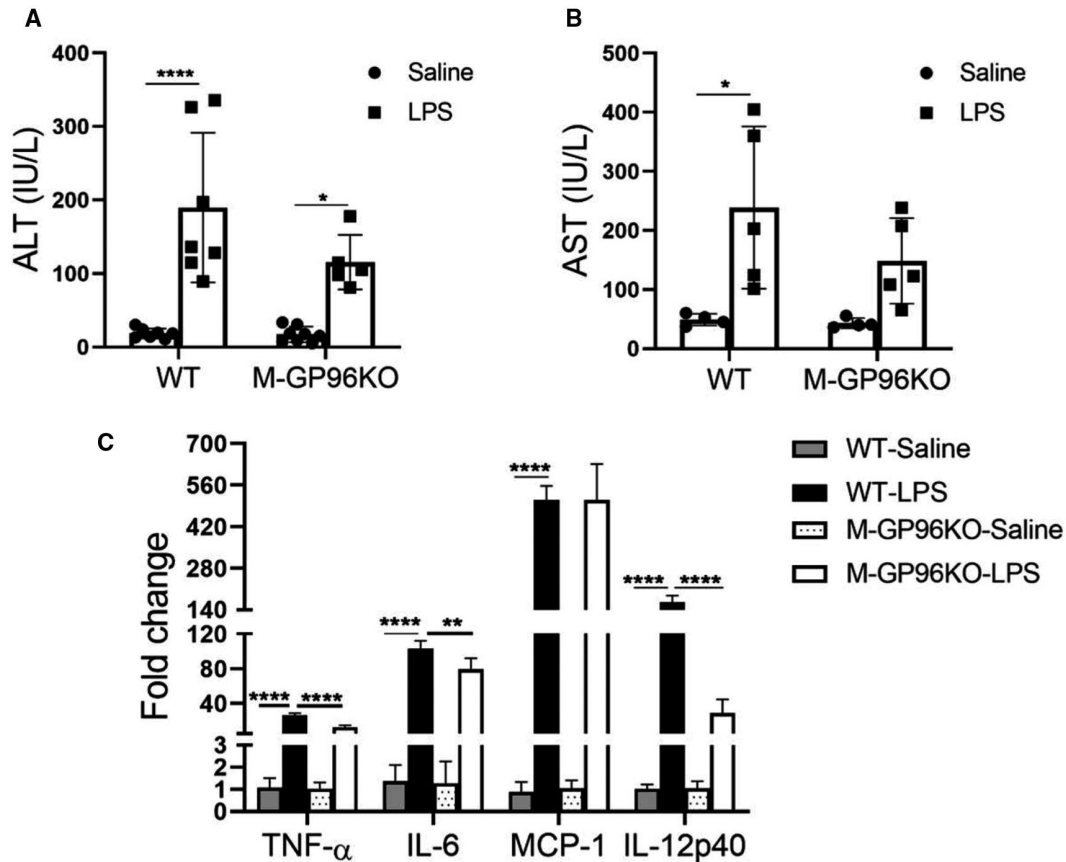


**FIG. 5.** Loss of myeloid-specific GP96 prevents LPS-induced liver injury and inflammation. Female WT and M-GP96KO mice were injected intraperitoneally with LPS (0.5 mg/kg body weight or saline ( $n = 4-8$ )). Serum was collected after 18 hours and subjected to analysis of ALT (A) and AST (B) and compared with the control group. (C) Livers were collected 2 hours after LPS injection, and liver cytokine mRNA was analyzed by RT-PCR. Data are presented as mean  $\pm$  SEM. \* $P < 0.05$ , \*\* $P < 0.01$ , \*\*\*\* $P < 0.0001$ .

Next, we used a model of low-dose endotoxin/LPS-induced liver injury to further explore the *in vivo* effect of LPS/TLR4 on liver macrophage activation and injury. *In vivo* LPS administration resulted in decreased serum ALT (Fig. 5A) and AST (Fig. 5B) in M-GP96KO mice compared with control mice. Because LPS-induced liver injury is largely mediated by pro-inflammatory cytokines, we estimated hepatic cytokine levels and found that LPS-induced

TNF- $\alpha$ , IL-6, and IL-12p40 cytokines were markedly reduced in livers of M-GP96KO mice (Fig. 5C). MCP-1 mRNA in LPS-injected M-GP96KO mice remained similar to control mice, which is interesting but not surprising as hepatocytes also produce MCP-1.<sup>(17)</sup> Overall, our data indicate that lack of myeloid-GP96 reduces pro-inflammatory response in the liver and favors anti-inflammatory responses likely contributing to reduced alcoholic liver injury.



## LOSS OF MYELOID-SPECIFIC GP96 INDUCES COMPENSATORY GRP78 INDUCTION IN ALCOHOLIC LIVER

Mounting evidence indicates that ER stress caused by accumulation of unfolded proteins contributes to ALD pathogenesis.<sup>(8,10,31)</sup> To identify whether deletion of ER resident chaperone GP96 affects ER stress, we analyzed the relative mRNA and protein abundance of representative ER stress-mediated UPR target genes. The mRNA expression of GRP78, ATF4, and CHOP was up-regulated in livers of alcohol-fed WT mice, while ATF6 $\alpha$ , sXBP-1, and usXBP-1 remained unchanged (Fig. 6A). Interestingly, GRP78, ATF4, and CHOP mRNA showed significant reduction, whereas sXBP-1 was induced significantly in alcohol-fed M-GP96KO mice livers. Increased GRP78 mRNA expression was reflected in isolated hepatocytes from alcohol-fed WT livers, which was reduced in alcohol-fed M-GP96KO livers (Fig. 6B). On the other hand, liver macrophages of alcohol-fed M-GP96KO mice exhibit significant increase in mRNA levels of GRP78, sXBP-1, and usXBP-1, whereas ATF4 mRNA was significantly reduced compared with alcohol-fed WT mice (Fig. 6C). The balance between spliced and unspliced XBP-1 was maintained in liver macrophages as compared with their respective WT alcohol-fed group (Supporting Fig. S4). Alcohol-induced CHOP protein show a decreasing trend in alcohol-fed M-GP96KO mice livers (Fig. 6D), whereas protein levels of cleaved ATF6 $\alpha$  and nuclear ATF4 were not significantly changed. These data suggest that loss of myeloid-specific GP96 in alcohol-fed mice leads to compensatory induction of GRP78, which is likely due to increased splicing of XBP-1 in liver macrophages.

## GP96 INHIBITION USING SPECIFIC INHIBITOR AND siRNA ABROGATES LPS-INDUCED PRO-INFLAMMATORY CYTOKINE PRODUCTION IN BMDMs

Studies from our group have reported that HSP90 inhibitors are potential therapeutic candidates in ALD.<sup>(6,22)</sup> Studies on targeted inhibition of ER paralog of HSP90 in ALD is not yet reported. To unravel the therapeutic significance of

inhibiting GP96, we assessed whether macrophages treated with GP96-specific inhibitor show reduced pro-inflammatory responses, similar to *in vivo* macrophages from alcohol-fed M-GP96KO mice. LPS-challenged BMDMs were treated with 0.5  $\mu$ M PU-WS13, a purine scaffold-based GP96 inhibitor. PU-WS13 is a small molecule whose selectivity for GP96 arises from its ability to bind to an allosteric pocket of GP96 that only partly overlaps with the ATP-binding pocket and is not accessible in the closely related paralog HSP90.<sup>(12)</sup> PU-WS13 treatment did not affect BMDM viability (Supporting Fig S5A). PU-WS13 treated BMDMs demonstrated significant attenuation in LPS-induced mRNA levels of pro-inflammatory cytokines TNF- $\alpha$ , IL-6, IL-1 $\beta$ , and MCP-1 (Fig. 7A-D). Complimentary to TNF- $\alpha$  mRNA level, the protein level was also significantly reduced in PU-WS13-treated BMDMs (Fig. 7E). We confirmed selective inhibition of HSP90 ER paralog by PU-WS13 in BMDMs by comparing the expression of cytoplasmic HSP70, induced by other HSP90 inhibitors, such as 17-DMAG.<sup>(6,18)</sup> Unlike 17-DMAG, which targets predominantly cytosolic pools of HSP90, resulting in HSP70 induction in the cytoplasm, PU-WS13 failed to induce HSP70 mRNA in LPS-exposed BMDMs (Supporting Fig. S5B), confirming specific inhibition of ER paralog HSP90B1, and not the cytosolic HSP90 isoform. Thus, inhibition of ER-specific HSP90B1/GP96 reduces inflammatory responses in macrophages, without affecting cytosolic HSP90. Next, we validated our results using GP96-specific siRNA-mediated knockdown in RAW 264.7 macrophages. Transient transfection of GP96 siRNA reduced LPS-induced TNF- $\alpha$  protein level in macrophages (Fig. 7F). Knockdown efficiency of GP96 by siRNA was confirmed by marked reduction of GP96 protein (Supporting Fig. S5C). These data confirm that ER-specific targeting of GP96 in primary macrophages inhibits pro-inflammatory cytokines, suggesting its potential as a therapeutic target to alleviate liver inflammation.

## Discussion

In the present study, we identified an important role of myeloid cell-specific ER resident HSP chaperone, GP96, in ALD. Increased expression

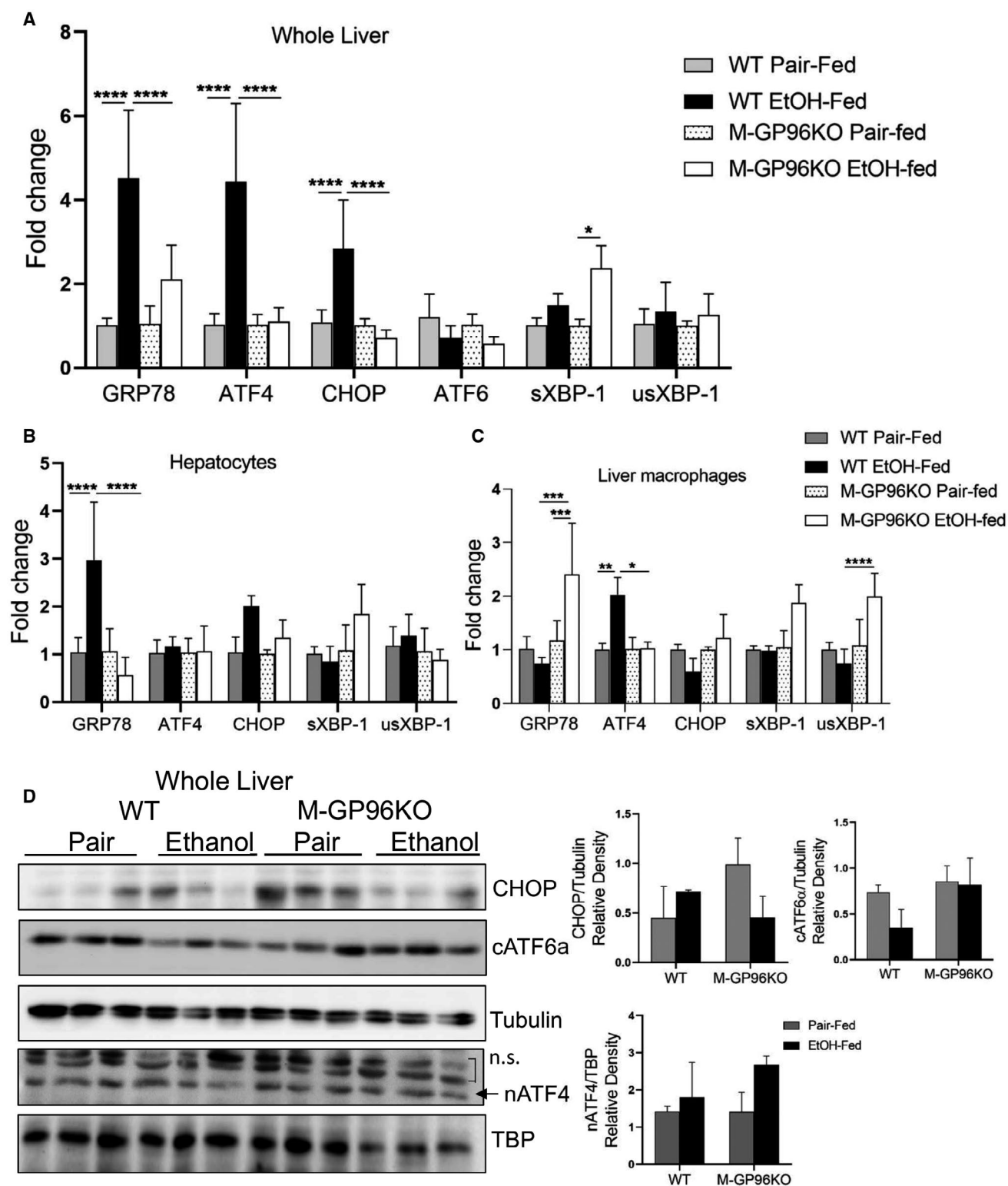


**FIG. 6.** Alcohol-induced ER stress mediators are reduced in M-GP96KO mice livers. Expression of genes associated with ER stress in whole-liver lysate (A), hepatocytes (B), and liver macrophages (C) isolated from pair-fed and alcohol-fed WT and M-GP96KO mice ( $n = 6-10$ ). (D) The protein levels of CHOP and cleaved ATF6 in whole-liver lysate and nuclear ATF4 in nuclear extract was analyzed by western blot. Tubulin and TBP were used as loading controls ( $n = 3$ ). Data are presented as mean  $\pm$  SEM. \* $P < 0.05$ , \*\* $P < 0.01$ , \*\*\*\* $P < 0.0001$ . Abbreviations: cATF6 $\alpha$ , cleaved ATF6 $\alpha$ ; nATF4, nuclear ATF4; n.s., nonspecific.

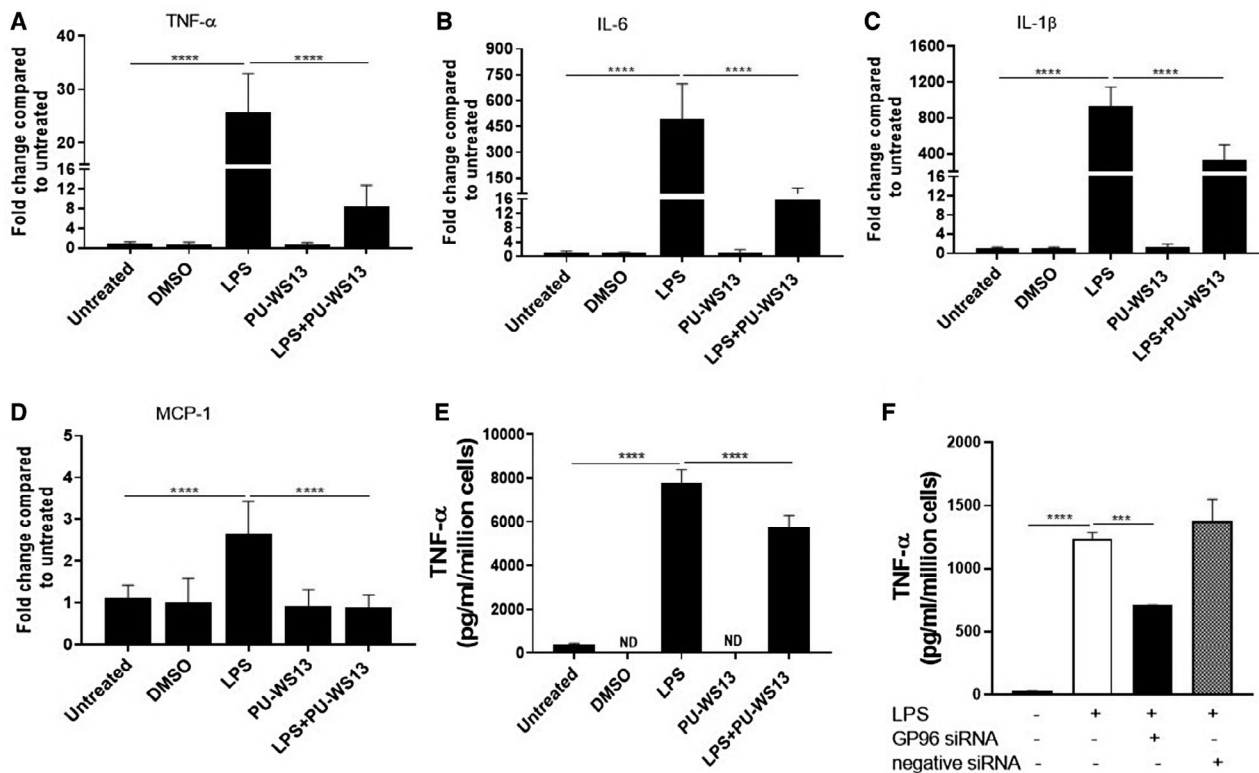


**FIG. 7.** Inhibition of GP96 using specific inhibitor PU-WS13 and siRNA reduces LPS-induced pro-inflammatory cytokine production. BMDMs were isolated from C57BL/6J mice and stimulated with LPS (100 ng/mL) for 2 hours and treated with PU-WS13 (0.5 μM) either alone for 2 hours or before LPS for 1 hour. DMSO-treated cells served as control group (n = 8). RT-PCR was carried out to evaluate the expression of TNF-α (A), IL-6 (B), IL-1β (C), and MCP-1 (D) and compared with the untreated group. (E) Culture supernatant was evaluated for secreted TNF-α by ELISA. (F) Murine macrophage RAW 264.7 cell line was transiently transfected with GP96 siRNA (100 nM) or negative control siRNA for 48 hours and stimulated with LPS for the final 6 hours. Secreted TNF-α level was measured in culture supernatant by ELISA. Data are presented as mean ± SEM. \*\*\**P* < 0.001, \*\*\*\**P* < 0.0001. Abbreviation: ND, not detected.

of GP96 occurs as a consequence of ER stress and downstream of the UPR.<sup>(10)</sup> Although studies have suggested its role in liver oncogenesis<sup>(25)</sup> and regeneration,<sup>(32)</sup> whether GP96 contributes to alcohol-mediated hepatic steatosis and inflammation is not known. Here, we show induction of GP96 in livers of patients with AH and in ALD murine models, suggesting its clinical relevance. Using murine models of experimental ALD, we found that myeloid-specific GP96 deficiency prevents liver injury, as indicated by reduced ALT and steatosis. Deficiency of GP96 in liver macrophages tips the balance in favor of FA oxidation genes with concomitant reduction in FA synthesis genes, contributing to decreased steatosis in livers of M-GP96KO mice. Loss of myeloid GP96 reduced circulating endotoxin, did not alter

Cyp2e1, and attenuated alcohol-induced liver pro-inflammatory cytokines TNF-α, IL-6, MCP-1 and IL-1β, whereas it increased anti-inflammatory cytokine, IL-10, and TGF-β. Furthermore, liver macrophages from alcohol-fed M-GP96KO mice exhibit compensatory induction of GRP78 and splicing of XBP-1, likely contributing to lower proteotoxic stress and reduced injury. Finally, our data show that pharmacological inhibition of GP96 using an ER permeable, specific inhibitor, and gene silencing using specific GP96 siRNA, exhibit reduced pro-inflammatory cytokines in murine macrophages. Taken together, we present evidence for pathophysiological significance of myeloid-specific GP96 during chronic alcohol-mediated liver inflammation and injury (Fig. 8).



The pathological significance of cytoplasmic and ER-associated proteostasis mediators in ALD are becoming increasingly recognized.<sup>(5)</sup> Induction of UPR signaling in hepatocytes during chronic alcohol-mediated liver injury has been identified.<sup>(8)</sup> However, the role of ER stress-mediated UPR in liver macrophage activation and inflammation in ALD is not completely understood. Here we observed an up-regulation of GP96 in livers of severe AH and explants from patients with AH as well as alcoholic cirrhosis, without changes in NAFLD and HCV livers. These data suggest that increased GP96 may specifically be linked to alcohol-induced inflammation and liver injury. Chronic alcohol feeding in mice led to GP96

induction in livers, and prominently in liver macrophages. Similarly, we observed induction of GP96 in murine primary macrophages exposed to alcohol *in vitro*. Based on these data, we investigated the role of myeloid GP96 on alcohol-mediated inflammation and liver injury. Previous studies have shown that alcohol-mediated ER stress induces another crucial ER chaperone, GRP78, in the liver.<sup>(8,33)</sup> In agreement, we noted increased GRP78 in livers of severe AH and explants from patients with AH. GRP78 induction was also noted in livers and hepatocytes, but not in macrophages of chronic alcohol-fed mice. Our results indicate clinical significance of myeloid GP96 in alcoholic liver injury.

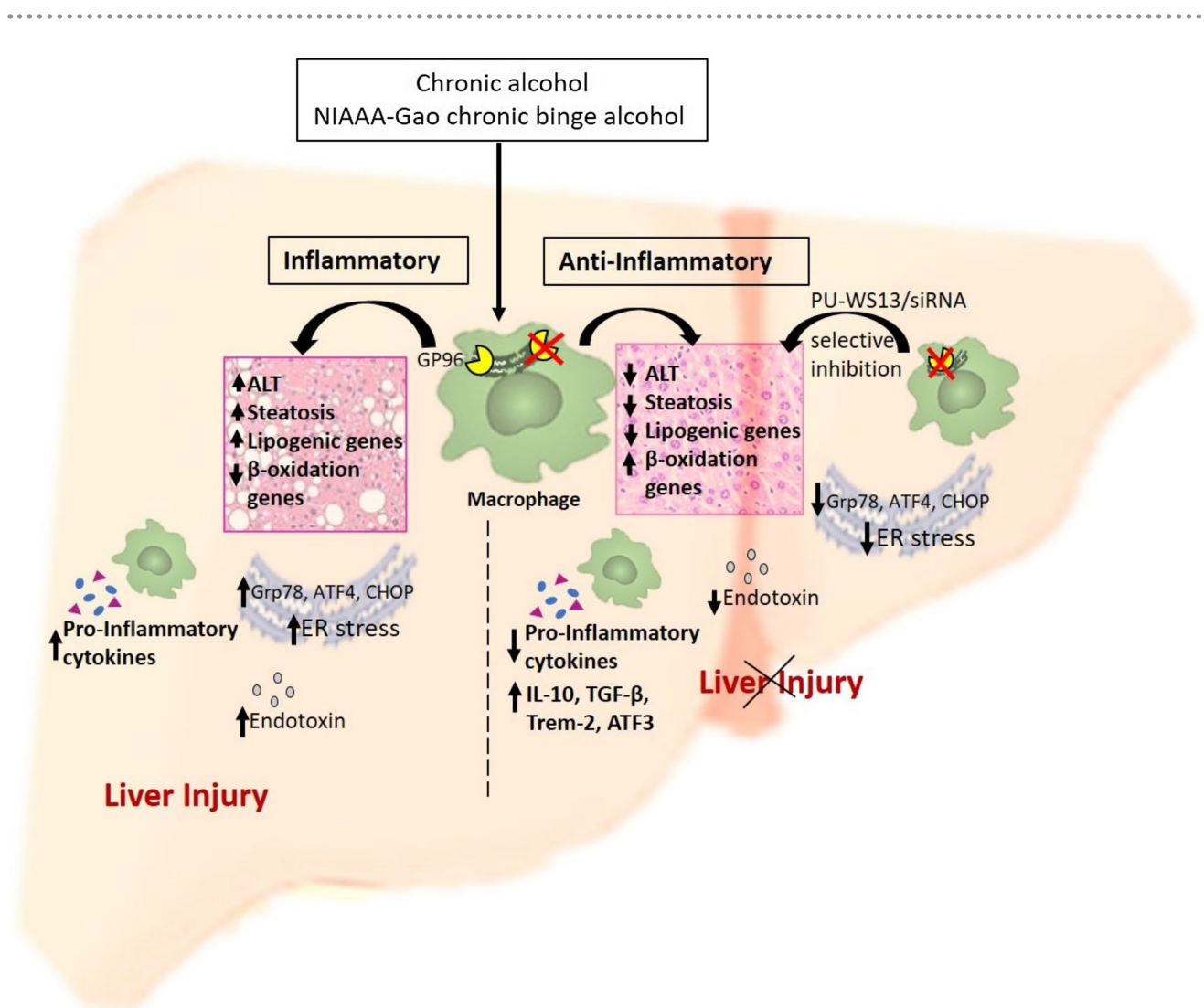


**FIG. 8.** Schematic representation depicting pathophysiological significance of macrophage-specific GP96 during chronic alcohol-mediated liver inflammation and injury.

Prolonged alcohol consumption induces steatosis and inflammatory mediators.<sup>(5,10)</sup> Here we show that mice lacking ER resident chaperone, GP96, in myeloid cells display protection from alcohol-mediated liver damage, as evidenced by diminished serum ALT and steatosis. It should be noted that in liver, GP96 is not only expressed by macrophages but also by hepatocytes. In our study, we focus on myeloid-specific GP96, and report its contribution to liver inflammation and injury. Excess fat accumulation in hepatocytes during ALD can occur due to *de novo* FA synthesis and impaired FA oxidation. In the present study, we found induction of nuclear PPAR- $\alpha$  protein and its target genes CPT1a, LCAD and MCAD, whereas lipogenic genes SREBPF1, SCD1, and FAS were reduced in alcohol-fed M-GP96KO mice. It is likely that crosstalk between hepatocytes and hepatic macrophages suggested previously in ALD<sup>(34)</sup> occurs in M-GP96KO mice. Pro-inflammatory cytokines such as liver-macrophage derived TNF- $\alpha$  can regulate lipogenesis through hepatic TNFR1.<sup>(35)</sup> Another study revealed crosstalk between KCs and hepatocytes regulating hepatic TG storage,<sup>(36)</sup> through an inhibitory effect of IL-1 $\beta$  on PPAR- $\alpha$  promoter activity, resulting in decreased FA oxidation.<sup>(36)</sup> In agreement with these reports, our data suggest that lack of GP96 in liver macrophages results in decreased pro-inflammatory cytokines (TNF- $\alpha$  and IL-1 $\beta$ ) and regulates lipid synthesis and oxidation genes in hepatocytes. Furthermore, it is likely that ER stress mediates hepatocyte-macrophage crosstalk pathways facilitated by GP96 in ALD, which will be studied in the future.

Alcohol-induced oxidative stress and hepatic inflammation are critical drivers of tissue injury during ALD.<sup>(37)</sup> Hepatic inflammation is triggered by binding of gut-derived pathogen-associated molecular patterns, such as LPS, to their specific TLRs expressed on liver macrophages, leading to production of pro-inflammatory cytokines.<sup>(38)</sup> Chronic alcohol-mediated increase in gut-derived, circulating endotoxin<sup>(39)</sup> was significantly reduced in M-GP96KO mice. Studies have identified a role for GP96 in intestinal epithelial homeostasis.<sup>(40)</sup> Interestingly, lack of GP96 in myeloid cells appears to prevent gut permeability, suggesting an important role for this chaperone in gut inflammation and permeability. The role of inflammation-mediated intestinal barrier dysfunction has been reported earlier in ALD<sup>(41)</sup> and will be

investigated in context with intestinal GP96 in the future. Chronic alcohol-induced hepatic inflammatory response and macrophage activation were reduced in M-GP96KO mice. Interestingly, anti-inflammatory cytokines IL-10 and TGF- $\beta$  were elevated in alcohol-fed M-GP96KO mice. Increased mRNA transcripts of TGF- $\beta$ , Trem-2, and ATF3 suggest transition from inflammatory to restorative phenotype of macrophages in liver of alcohol-fed M-GP96KO mice. *LysMCre*-mediated deletion of GP96 induced ATF3 protein, further supporting that phenotypic change in liver macrophages may be facilitated by loss of GP96. Detailed phenotypic characteristics of these macrophages will be characterized in our future studies. Pathophysiological role of macrophage GP96 was also noted in a model of endotoxin-mediated liver injury, in which M-GP96KO mice showed lower serum ALT and inflammatory responses. Previous studies have reported that GP96 is a master chaperone for maturation and functioning of TLRs.<sup>(11)</sup> Our findings support the notion that in the absence of macrophage GP96, cell-surface expression of TLR4 is affected, resulting in blunted inflammatory response. It is known that inhibition of liver macrophages or blocking circulating endotoxin alleviates ALD in animal experiments.<sup>(1,42)</sup> Our data suggest that targeting GP96 in macrophages inhibits endotoxin responses, which could be beneficial in curbing the inflammatory response during ALD.

Alcohol consumption leads to accumulation of misfolded proteins, disrupts ER homeostasis, and induces UPR in both primary hepatocyte cultures and in mouse livers.<sup>(8,43)</sup> In line with this, we observed elevated expression of ER chaperones, GRP78 and GP96, as well as ATF4 and CHOP, two major downstream mediators of PERK (PKR-like endoplasmic reticulum localized kinase) pathway in murine alcoholic liver. UPR signaling in alcoholic liver is induced to cope with increased proteotoxic and lipotoxic burden. Our data show that myeloid GP96 modulates ER stress in alcoholic livers, likely favoring lower proteotoxic stress. Interestingly, we found reduced ATF4 expression, whereas GRP78 expression was elevated in isolated liver macrophages from alcohol-fed M-GP96KO mice. Previous studies showed that ATF4 can directly regulate IL-6 and CCL2 expression in macrophages.<sup>(44,45)</sup> It is likely that reduced IL-6 and CCL2 in alcohol-fed M-GP96KO is due to decreased ATF4. Moreover, increased GRP78 in alcoholic macrophages

may occur due to compensatory induction of another chaperone due to deficiency of GP96,<sup>(46)</sup> suggesting that increased GRP78 retains cellular homeostasis and relieves ER stress in M-GP96KO mice. Increased splicing of XBP-1 in liver macrophages of alcohol-fed M-GP96KO mice suggest that activation of this pathway is likely responsible for the higher expression of GRP78. Detailed analysis of specific UPR pathway in M-GP96KO alcoholic livers leading to GRP78 induction will be investigated in the future.

Because myeloid-specific GP96 deficiency reduces inflammation, we used specific GP96 siRNA and pharmacological GP96-specific inhibitor, PU-WS13,<sup>(12,13)</sup> to evaluate macrophage-mediated pro-inflammatory responses. Consistent with our *in vivo* data, inhibition of GP96 using PU-WS13 or siRNA significantly decreased LPS-mediated pro-inflammatory cytokine production in primary macrophages. Thus, future exploration of targeting GP96 using specific inhibitors *in vivo* to alleviate alcohol-induced liver damage deserves further investigation.

In summary, we report an important pathophysiological role for myeloid-specific ER resident HSP family chaperone GP96 in ALD. The contribution of ER stress mediators have been implicated in alcohol-related hepatocyte apoptosis,<sup>(47)</sup> hepatocellular injury<sup>(48)</sup> and hyperhomocysteinemia.<sup>(8)</sup> Using different models of alcohol-mediated and endotoxin-mediated liver injury, we identified that selective macrophage GP96 deletion protected mice from liver injury and inflammation. Our findings on the pathophysiological significance of macrophage GP96 adds to our understanding of the mechanisms associated with ALD and have implications in developing therapeutics. In fact, mutations in GP96 can reduce macrophage activation while retaining antigen presentation activity<sup>(49)</sup> to combat infections in ALD. Although complete inhibition of liver macrophage activation and inflammatory responses in ALD can be a clinical limitation, targets that promote recovery/restorative phenotype to facilitate elimination of damaging triggers in the liver could be beneficial. Our ongoing studies are focused on investigating the effect of GP96 deletion in myeloid cells on selective induction of anti-inflammatory or restorative macrophage phenotype. We are also assessing the involvement of upstream mediators of UPR pathways such as PERK, eukaryotic initiation factor 2 $\alpha$ , and inositol-requiring enzyme-1 $\alpha$  in macrophage activation during alcoholic

liver injury. Overall, our studies indicate that inhibition of myeloid GP96 may represent an attractive therapeutic strategy in the management of ALD.

*Acknowledgment:* The authors thank the UMass Medical School Flow Cytometry Core Facility.

## REFERENCES

- 1) Mandrekar P, Bataller R, Tsukamoto H, Gao B. Alcoholic hepatitis: translational approaches to develop targeted therapies. *Hepatology* 2016;64:1343-1355.
- 2) Morimoto RI. Cells in stress: transcriptional activation of heat shock genes. *Science* 1993;259:1409-1410.
- 3) Muralidharan S, Ambade A, Fulham MA, Deshpande J, Catalano D, Mandrekar P. Moderate alcohol induces stress proteins HSF1 and hsp70 and inhibits proinflammatory cytokines resulting in endotoxin tolerance. *J Immunol* 2014;193:1975-1987.
- 4) Csermely P, Schnaider T, Soti C, Prohászka Z, Nardai G. The 90-kDa molecular chaperone family: structure, function, and clinical applications. A comprehensive review. *Pharmacol Ther* 1998;79:129-168.
- 5) Kaplowitz N, Ji C. Unfolding new mechanisms of alcoholic liver disease in the endoplasmic reticulum. *J Gastroenterol Hepatol* 2006;21(Suppl 3):S7-S9.
- 6) Ambade A, Catalano D, Lim A, Kopoyan A, Shaffer SA, Mandrekar P. Inhibition of heat shock protein 90 alleviates steatosis and macrophage activation in murine alcoholic liver injury. *J Hepatol* 2014;61:903-911.
- 7) Rachidi S, Sun S, Wu BX, Jones E, Drake RR, Ogretmen B, et al. Endoplasmic reticulum heat shock protein gp96 maintains liver homeostasis and promotes hepatocellular carcinogenesis. *J Hepatol* 2015;62:879-888.
- 8) Ji C, Kaplowitz N. Betaine decreases hyperhomocysteinemia, endoplasmic reticulum stress, and liver injury in alcohol-fed mice. *Gastroenterology* 2003;124:1488-1499.
- 9) Maiers JL, Malhi H. Endoplasmic reticulum stress in metabolic liver diseases and hepatic fibrosis. *Semin Liver Dis* 2019;39:235-248.
- 10) Guo B, Li Z. Endoplasmic reticulum stress in hepatic steatosis and inflammatory bowel diseases. *Front Genet* 2014;5:242.
- 11) Yang Y, Liu B, Dai J, Srivastava PK, Zammit DJ, Lefrançois L, et al. Heat shock protein gp96 is a master chaperone for toll-like receptors and is important in the innate function of macrophages. *Immunity* 2007;26:215-226.
- 12) Patel PD, Yan P, Seidler PM, Patel HJ, Sun W, Yang C, et al. Paralog-selective Hsp90 inhibitors define tumor-specific regulation of HER2. *Nat Chem Biol* 2013;9:677-684.
- 13) Yan P, Patel HJ, Sharma S, Corben A, Wang T, Panchal P, et al. Molecular stressors engender protein connectivity dysfunction through aberrant N-glycosylation of a chaperone. *Cell Rep* 2020;31:107840.
- 14) Argemi J, Latasa MU, Atkinson SR, Blokhin IO, Massey V, Gue JP, et al. Defective HNF4 $\alpha$ -dependent gene expression as a driver of hepatocellular failure in alcoholic hepatitis. *Nat Commun* 2019;10:3126.
- 15) Mathurin P, Moreno C, Samuel D, Dumortier J, Salleron J, Durand F, et al. Early liver transplantation for severe alcoholic hepatitis. *N Engl J Med* 2011;365:1790-1800.
- 16) Fulham MA, Ratna A, Gerstein RM, Kurt-Jones EA, Mandrekar P. Alcohol-induced adipose tissue macrophage phenotypic switching is independent of myeloid Toll-like receptor 4 expression. *Am J Physiol Cell Physiol* 2019;317:C687-C700.



- 17) Mandrekar P, Ambade A, Lim A, Szabo G, Catalano D. An essential role for monocyte chemoattractant protein-1 in alcoholic liver injury: regulation of proinflammatory cytokines and hepatic steatosis in mice. *Hepatology* 2011;54:2185-2197.
- 18) Ambade A, Catalano D, Lim A, Mandrekar P. Inhibition of heat shock protein (molecular weight 90 kDa) attenuates proinflammatory cytokines and prevents lipopolysaccharide-induced liver injury in mice. *Hepatology* 2012;55:1585-1595.
- 19) Bertola A, Mathews S, Ki SH, Wang H, Gao B. Mouse model of chronic and binge ethanol feeding (the NIAAA model). *Nat Protoc* 2013;8:627-637.
- 20) **Tencerova M, Auouadi M**, Vangala P, Nicoloro SM, Yawe JC, Cohen JL, et al. Activated Kupffer cells inhibit insulin sensitivity in obese mice. *FASEB J* 2015;29:2959-2969.
- 21) Mandrekar P, Catalano D, Szabo G. Inhibition of lipopolysaccharide-mediated NFkappaB activation by ethanol in human monocytes. *Int Immunol* 1999;11:1781-1790.
- 22) Choudhury A, Bullock D, Lim A, Argemi J, Orning P, Lien E, et al. Inhibition of HSP90 and activation of HSF1 diminish macrophage NLRP3 inflammasome activity in alcohol-associated liver injury. *Alcohol Clin Exp Res* 2020;44:1300-1311.
- 23) **Patel HJ, Patel PD, Ochiana SO, Yan P, Sun W, Patel MR**, et al. Structure-activity relationship in a purine-scaffold compound series with selectivity for the endoplasmic reticulum Hsp90 paralogue Grp94. *J Med Chem* 2015;58:3922-3943.
- 24) Ji C, Kaplowitz N, Lau MY, Kao E, Petrovic LM, Lee AS. Liver-specific loss of glucose-regulated protein 78 perturbs the unfolded protein response and exacerbates a spectrum of liver diseases in mice. *Hepatology* 2011;54:229-239.
- 25) **Ji F, Zhang Y, Zhu ZB**, Guo Y, Shen SL, Cao QH, et al. Low levels of glycoprotein 96 indicate a worse prognosis in early-stage hepatocellular carcinoma patients after hepatectomy. *Hum Pathol* 2019;86:193-202.
- 26) Mandrekar P, Bala S, Catalano D, Kodys K, Szabo G. The opposite effects of acute and chronic alcohol on lipopolysaccharide-induced inflammation are linked to IRAK-M in human monocytes. *J Immunol* 2009;183:1320-1327.
- 27) You M, Fischer M, Deeg MA, Crabb DW. Ethanol induces fatty acid synthesis pathways by activation of sterol regulatory element-binding protein (SREBP). *J Biol Chem* 2002;277:29342-29347.
- 28) Cohen JI, Chen X, Nagy LE. Redox signaling and the innate immune system in alcoholic liver disease. *Antioxid Redox Signal* 2011;15:523-534.
- 29) **Liu B, Yang Y**, Qiu Z, Staron M, Hong F, Li Y, et al. Folding of toll-like receptors by the HSP90 paralogue gp96 requires a substrate-specific cochaperone. *Nat Commun* 2010;1:79.
- 30) Perugorria MJ, Esparza-Baquer A, Oakley F, Labiano I, Korosec A, Jais A, et al. Non-parenchymal TREM-2 protects the liver from immune-mediated hepatocellular damage. *Gut* 2019;68:533-546.
- 31) Ji C. Dissection of endoplasmic reticulum stress signaling in alcoholic and non-alcoholic liver injury. *J Gastroenterol Hepatol* 2008;23(Suppl 1):S16-S24.
- 32) Radosevic-Stasic B, Jakovac H, Grebic D, Trobonjaca Z, Mrakovcic-Sutic I, Cuk M. Heat shock protein Gp96 as potential regulator of morphostasis after partial hepatectomy in mice. *Curr Aging Sci* 2012;5:254-262.
- 33) Ji C, Chan C, Kaplowitz N. Predominant role of sterol response element binding proteins (SREBP) lipogenic pathways in hepatic steatosis in the murine intragastric ethanol feeding model. *J Hepatol* 2006;45:717-724.
- 34) Kisseleva T, Brenner DA. The crosstalk between hepatocytes, hepatic macrophages, and hepatic stellate cells facilitates alcoholic liver disease. *Cell Metab* 2019;30:850-852.
- 35) **Wandrer F, Liebig S**, Marhenke S, Vogel A, John K, Manns MP, et al. TNF-receptor-1 inhibition reduces liver steatosis, hepatocellular injury and fibrosis in NAFLD mice. *Cell Death Dis* 2020;11:212.
- 36) Stienstra R, Saudale F, Duval C, Keshtkar S, Groener JE, van Rooijen N, et al. Kupffer cells promote hepatic steatosis via interleukin-1beta-dependent suppression of peroxisome proliferator-activated receptor alpha activity. *Hepatology* 2010;51:511-522.
- 37) Seki E, Brenner DA. Toll-like receptors and adaptor molecules in liver disease: update. *Hepatology* 2008;48:322-335.
- 38) Seitz HK, Batailler R, Cortez-Pinto H, Gao B, Gual A, Lackner C, et al. Alcoholic liver disease. *Nat Rev Dis Primers* 2018;4:16.
- 39) **Bala S, Marcos M**, Gattu A, Catalano D, Szabo G. Acute binge drinking increases serum endotoxin and bacterial DNA levels in healthy individuals. *PLoS One* 2014;9:e96864.
- 40) Liu B, Staron M, Hong F, Wu BX, Sun S, Morales C, et al. Essential roles of grp94 in gut homeostasis via chaperoning canonical Wnt pathway. *Proc Natl Acad Sci U S A* 2013;110:6877-6882.
- 41) Chen P, Starkel P, Turner JR, Ho SB, Schnabl B. Dysbiosis-induced intestinal inflammation activates tumor necrosis factor receptor I and mediates alcoholic liver disease in mice. *Hepatology* 2015;61:883-894.
- 42) Adachi Y, Bradford BU, Gao W, Bojes HK, Thurman RG. Inactivation of Kupffer cells prevents early alcohol-induced liver injury. *Hepatology* 1994;20:453-460.
- 43) **Ramirez T, Longato L**, Dostalek M, Tong M, Wands JR, de la Monte SM. Insulin resistance, ceramide accumulation and endoplasmic reticulum stress in experimental chronic alcohol-induced steatohepatitis. *Alcohol Alcohol* 2013;48:39-52.
- 44) Liu B, Chen P, Xi D, Zhu H, Gao Y. ATF4 regulates CCL2 expression to promote endometrial cancer growth by controlling macrophage infiltration. *Exp Cell Res* 2017;360:105-112.
- 45) Iwasaki Y, Suganami T, Hachiya R, Shirakawa I, Kim-Saijo M, Tanaka M, et al. Activating transcription factor 4 links metabolic stress to interleukin-6 expression in macrophages. *Diabetes* 2014;63:152-161.
- 46) Song L, Kim DS, Gou W, Wang J, Wang P, Wei Z, et al. GRP94 regulates M1 macrophage polarization and insulin resistance. *Am J Physiol Endocrinol Metab* 2020;318:E1004-E1013.
- 47) Iracheta-Vellve A, Petrasek J, Gyongyosi B, Satishchandran A, Lowe P, Kodys K, et al. Endoplasmic reticulum stress-induced hepatocellular death pathways mediate liver injury and fibrosis via stimulator of interferon genes. *J Biol Chem* 2016;291:26794-26805.
- 48) Sanz-Garcia C, Poulsen KL, Bellos D, Wang H, McMullen MR, Li X, et al. The non-transcriptional activity of IRF3 modulates hepatic immune cell populations in acute-on-chronic ethanol administration in mice. *J Hepatol* 2019;70:974-984.
- 49) Liu W, Chen M, Li X, Zhao B, Hou J, Zheng H, et al. Interaction of toll-like receptors with the molecular chaperone gp96 is essential for its activation of cytotoxic T lymphocyte response. *PLoS One* 2016;11:e0155202.

Author names in bold designate shared co-first authorship.

## Supporting Information

Additional Supporting Information may be found at [onlinelibrary.wiley.com/doi/10.1002/hep4.1713/supinfo](https://onlinelibrary.wiley.com/doi/10.1002/hep4.1713/supinfo).